

# Terahertz study of 1,3,5-trinitro-s-triazine by time-domain and Fourier transform infrared spectroscopy

Feng Huang, Brian Schulkin, Hakan Altan, John F. Federici,<sup>a)</sup> and Dale Gary  
*Department of Physics, New Jersey Institute of Technology, Newark, New Jersey 07102*

Robert Barat

*Otto York Department of Chemical Engineering, New Jersey Institute of Technology,  
 Newark, New Jersey 07102*

David Zimdars

*Picometrix, Inc., 2925 Boardwalk, Ann Arbor, Michigan 48104-6765*

Minghan Chen and D. B. Tanner

*Department of Physics, University of Florida, Gainesville, Florida 32611-8440*

(Received 9 April 2004; accepted 7 October 2004)

This letter describes the use of THz time-domain spectroscopy (TDS) applied in transmission to the secondary explosive 1,3,5 trinitro-s-triazine. Samples were also subjected to Fourier transform infrared spectroscopy over the same range for comparison. A detailed spectroscopy study is presented. General agreement between results from both methods confirms the absorption features found. A comparison study with computer molecular simulations shows that THz-TDS is sensitive to collective modes or vibrational modes of material. © 2004 American Institute of Physics. [DOI: 10.1063/1.1829793]

The recent availability of sources and detectors of THz radiation has resulted in increased interest in THz technology.<sup>1,2</sup> Since many nonmetallic and nonpolar materials are transparent to THz radiation, there has been an increased interest in applying THz spectroscopy to the detection of concealed explosives, and chemical and biological agents. Globus *et al.*<sup>3</sup> experimentally characterized the THz vibrational spectra of deoxyribonucleic acid macromolecules. Woolard *et al.*<sup>4</sup> offered sensitivity limits and discrimination capability for THz transmission spectroscopy for biological agent detection. Choi *et al.*<sup>5</sup> measured transmission THz spectra for various organic species, such as flour and an anthrax simulant. Kemp *et al.*<sup>6</sup> showed that several common energetic (explosive) materials including 1,3,5 trinitro-s-triazine (RDX) have characteristic spectral features in this range. THz time-domain spectroscopy (TDS), Fourier transform infrared (FTIR) experiments, and computer simulation of the far-infrared spectra of organic molecules show vibrational features associated with intermolecular hydrogen bond relative motions.<sup>7-9</sup>

In this letter, we summarize our investigation into THz spectroscopy as a method to identify and distinguish spectral features of RDX. To this end, we investigated the connection between the low-frequency vibrational or phonon modes and molecular conformation of these molecules through THz spectroscopy,<sup>10</sup> with the help of computer simulation. In addition, FTIR spectroscopy was used to confirm and extend the time domain THz results.

We use a THz time-domain spectrometer setup with an optical layout as in Fig. 1. Low-temperature GaAs photoconductive antennas (emitter and detector) are driven by pulses of 80 fs duration from a Ti:Sapphire oscillator. Each pair of 20  $\mu\text{m}$  wide antenna electrodes are spaced by 50  $\mu\text{m}$  and biased by an external voltage of  $\sim 5\text{--}15$  V. The carriers ex-

cited by the laser pulse are accelerated by the strong bias field, thereby emitting an electrical transient. The duration of the THz radiation is limited by the carrier lifetime, which is in the order of 500 fs. When gated by the fs laser pulse, a current proportional to the electrical transient is measured using a lock-in amplifier, referenced to a signal generator synchronous output that also provides the emitter biasing voltage. The THz beam is focused to a nearly frequency-independent spot size of  $\sim 1$  mm where the sample is placed. A nearby aperture is for reference scan. The setup is currently functional in the range from 0.1 to 1.6 THz ( $3.3\text{--}53\text{ cm}^{-1}$ ) for this study.

In Fig. 2, the transmission spectra of the pulses passing through RDX sample and an aperture are shown, illustrating a signal-to-noise ratio (SNR) of up to  $10^6$  and a high repeatability over the spectral range with fingerprint features. The transmitted sample spectra are normalized by a corresponding blank (aperture) spectra. The strong broad absorption at  $\sim 0.8$  THz increases with the RDX sample thickness con-

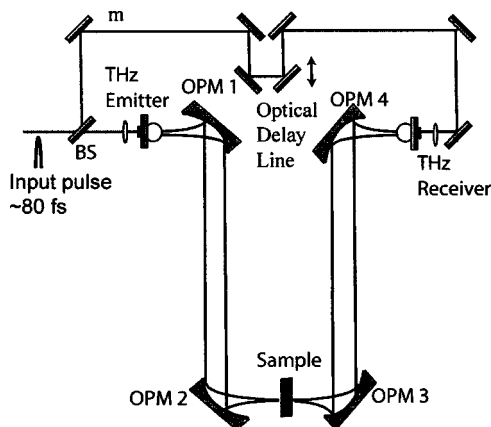


FIG. 1. Schematic setup of the THz-TDS. OPM is optical parabolic mirror, BS is beam splitter, and m is mirror.

<sup>a)</sup>Electronic mail: federici@adm.njit.edu

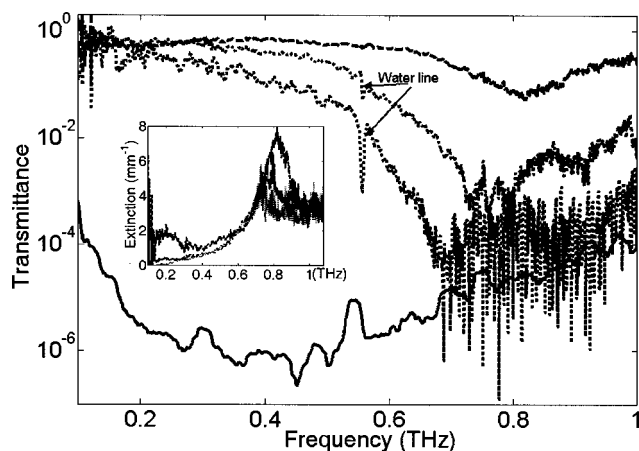


FIG. 2. The spectra of RDX. The first three lines correspond to the transmission lines of RDX with thicknesses of 0.1 mm, 1 mm, and 2 mm. The repeatability of the absorption feature at the 0.8 THz in accordance with the Beer–Lambert Law shows that the 0.8 THz is not, for example, a spectral artifact resulting from multiple reflections. For the thicker samples (1 mm and 2 mm), the shift of absorption center frequency to longer wavelengths is a spectroscopy artifact due to excessive absorption in the vicinity of resonance. For the thinnest sample, an equation takes into account of that multiple reflection is needed (see Ref. 11). The noise background is shown as the last line.

tent with the Beer–Lambert Law. The narrow water absorption lines indicate the variation of the water vapor level between the aperture-only scan and the material scan.

The application of THz-TDS to spectroscopy of organics, such as to RDX, is vulnerable to artifacts due to the fine spectral resolution ( $\sim 1 \text{ cm}^{-1}$  or  $0.03 \text{ THz}$ ) required. There are several experimental artifacts to be considered such as multiple reflections within the sample, multiple reflections between the sample, its holder and multiple reflections from the system, etc.<sup>4</sup> A low SNR can result when the transmitted THz light is attenuated by scattering of particles which are comparable in size to the THz wavelength. Careful sample preparation was found to be critical in gathering reliable data. Here, the desired thickness of RDX powder is held between two thin polyethylene films. The grain size of RDX is on the order of  $\mu\text{m}$ , therefore scattering is not a dominant factor compare to the THz wavelength ( $300 \mu\text{m}$ ).

FTIR is considered a standard spectroscopy tool down to  $100 \text{ cm}^{-1}$ . Compared to the THz-TDS technique, however, in its usual single beam setup, FTIR lacks direct phase information. The FTIR light sources are usually broadband black-body radiators instead of narrow coherent sources, and its SNR in the THz range is usually less than what is available in dedicated THz technologies. Comparison between the spectra obtained by FTIR and THz-TDS, however, is worthwhile. The two techniques yielded similar results (see Fig. 3) in spite of operational differences including light polarization state, source coherence, and intensity.

In order to better understand our THz-TDS spectra, we compare our THz spectra of RDX with a SPARTAN *ab initio* molecular simulations<sup>12</sup> study using the 6-311+G\*\* basis set and density function theory. From the molecular simulations, major spectral features should not exist below 1 THz for known molecular conformations of RDX. *Ab initio* calculation of the vibration modes of one single RDX molecule compared well with the experimental FTIR data beyond  $600 \text{ cm}^{-1}$ .<sup>12</sup>

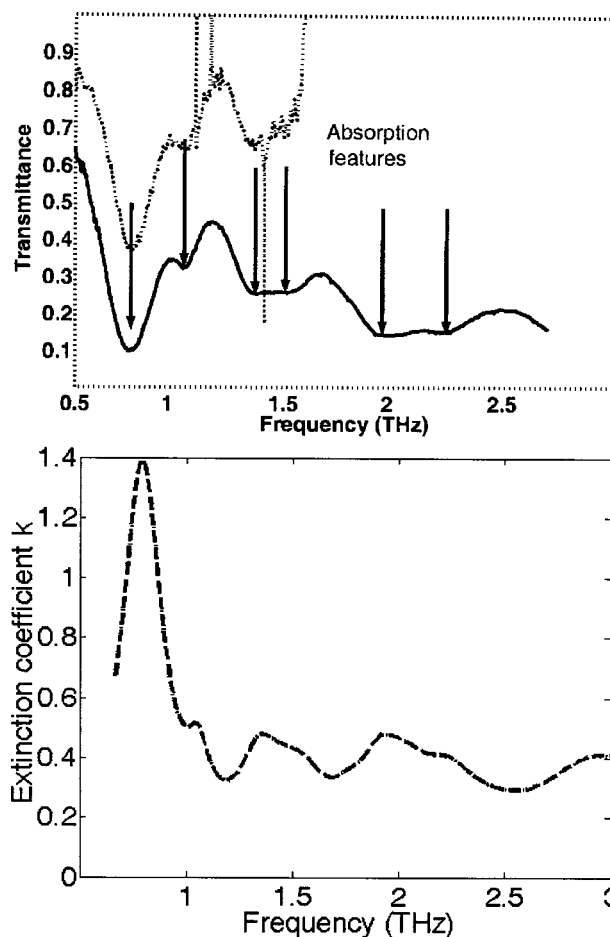


FIG. 3. Comparison study of transmission spectra of RDX using THz-TDS (dashed line) and FTIR (solid line). The downward arrows indicate the spectral peaks. The sharper features in both spectra are from water absorption. THz-TDS used a lower concentration of RDX as the sample. The curve fitting result is shown in the bottom (no observed discrepancy between the experiment and curve fit result).

The observed 0.8 THz feature (1.05 THz is not repeated by another group)<sup>6</sup> (see Fig. 3) is interesting since it does not appear to correspond to an inherent molecular vibrational mode. It is therefore reasonable to attribute this significant absorption feature at  $\sim 0.8 \text{ THz}$  to interactions between the RDX molecules. Possible explanations include molecular conformations [e.g., partial rotations of the nitro ( $-\text{NO}_2$ ) groups], a weak hydrogen bond between two RDX mol-

TABLE I. Experimental resonance frequencies for RDX with extracted Lorentzian line shape parameters from the data of Fig. 3. In comparing the experimental and theoretical values,  $a_j$  and  $A$  can be compared on a relative basis.

Peak	Experimental			Theoretical ( $\alpha$ -phase) <sup>a</sup>	
	$\omega_j$ (THz)	$a_j$ (arb. U.)	$\omega_j$ (THz)	$\omega_0$ (THz)	$A$ (arb. U.)
1	0.79	1.21	0.11		
2	1.05	0.16	0.06		
3	1.34	0.23	0.09	1.32	2
4	1.44	0.11	0.11		
5	1.56	0.13	0.11		
6	1.77	0.06	0.12	1.8	11
7	1.92	0.20	0.11	1.89	18

<sup>a</sup>See Ref. 12.

ecules, or a partial rotation of the RDX molecule. Since the grain size of RDX is in the order of microns, one can estimate the cutoff phonon wavelength at the lower frequency to be twice times the boundary size  $\sim 5 \mu\text{m}$ . The phonon absorption is therefore excluded. It is more likely to arise from nearest molecule-to-molecule interactions as listed above, or from single molecule librations which are difficult to model accurately due to a large number of atoms involved.

Whatever the exact cause, the 0.8 THz absorption suggests a strong intermolecular phonon absorption that can be modeled by the dielectric harmonic oscillator. Using this model, the physical parameters from the observed spectra can be extracted through a sum of resonance lines. First, a Lorentzian line shape for spectral signal  $S(\omega)$  is assumed:

$$S(\omega) = S_{nr}(\omega) + \sum_j \frac{a_j}{1 + i(\omega - \omega_j)/\sigma_j}, \quad (1)$$

where  $a_j$ ,  $\omega_j$ , and  $\sigma_j$  are the oscillator strength, the frequency, and linewidth of the  $j$ th absorption mode, respectively, and  $S_{nr}$  is the nonresonant background contribution. The scattered signal is proportional to  $S^2$ .

From the calculated oscillator strength, an estimation of the intermolecular interaction can be obtained. The nonresonance contribution is a monotonic increasing function of the frequency, which can be fitted by an exponential decay function according to Beer's Law. Equation (1) can be curve or peak fitted using a commercial available program such as PEAKFIT®. Curve fitting of the FTIR curve of Fig. 3 using the Lorentzian line shape of Eq. (1) is shown to the right of Fig. 3, and the parameters are shown in Table I.

From Table I, one finds that peak 1 at 0.8 THz (absorption peak 1) has much larger oscillator strength than the other peaks, suggesting that feature 1 is a fundamentally different phenomenon from the others. We assign peaks 3–7 to be vibrational modes: The center THz frequencies of these peaks are very close to the calculated vibrational modes of the RDX, as shown in the Table I.

THz-TDS provides additional features, such as a net phase profile of the absorption materials, which could determine how much dispersion exists at a certain resonance location. The seven spectra features indicated in the Fig. 3 can then be used as spectral characteristics for the identification of the RDX. In addition, the most distinguishable absorption feature at 0.8 THz may be used as an indication of intermolecular interaction.

In conclusion, we have successfully applied the THz-TDS to study RDX in the THz and it has produced an agreeable result with FTIR in far-infrared regime. Comparison with molecular simulations suggests that the 0.8 THz absorption peak is due to intermolecular action. The results suggest that THz spectroscopy is a potentially important scientific tool in understanding the collective motion and conformational status of molecules.

The authors gratefully acknowledge the funding support of the US Army SBIR program (Contract No. DAAD19-03-C-0137) and TSWG-ED (Contract No. N41756-04-C-4163).

<sup>1</sup>D. M. Mittleman, *Sensing with Terahertz Radiation* (Springer, Berlin, 2002).

<sup>2</sup>D. W. van der Weide, *Terahertz Sources and Systems*, edited by R. E. Miles *et al.*, eds. (Kluwer, The Netherlands, 2001), pp. 301–314.

<sup>3</sup>T. Globus, L. Dolmatova-Werbos, D. L. Woolard, A. C. Samuels, B. Gelmont, and M. Bykhovskaia, *Proceedings of the 2001 ISSSR* (2001).

<sup>4</sup>D. Woolard, T. Globus, E. Brown, L. Werbos, B. Gelmont, and A. Samuels, *Proceedings of the Fifth Joint Conference on Standoff Detection for Chemical and Biological Defense* (2001).

<sup>5</sup>M. K. Choi, K. Taylor, A. Bettermann, and D. W. van der Weide, *Phys. Med. Biol.* **47**, 3777 (2002).

<sup>6</sup>M. C. Kemp, P. F. Taday, B. E. Cole, J. A. Cluff, A. J. Fitzgerald, and W. R. Tribe, *Proc. SPIE* **5070**, 44 (2003).

<sup>7</sup>J. Xu, H. Liu, R. Kersting, and X. Zhang, *Proc. SPIE* **5070**, 17 (2003).

<sup>8</sup>T. A. Heimer and E. J. Heilweil, *Bull. Chem. Soc. Jpn.* **75**, 899 (2002).

<sup>9</sup>D. L. Woolard, T. Koscica, D. L. Rhodes, H. L. Cui, R. A. Pastore, J. O. Jensen, J. L. Jensen, W. R. Loerop, R. H. Jacobsen, D. M. Mittleman, and M. C. Nuss, *J. Appl. Toxicol.* **17**, 243 (1997).

<sup>10</sup>P. Han, G. Cho, and X. Zhang, *Opt. Lett.* **25**, 242 (2000).

<sup>11</sup>L. Kellner, *Z. Phys.* **56**, 212 (1929).

<sup>12</sup>B. M. Rice and G. F. Chabalowski, *J. Phys. Chem. A* **101**, 8720 (1997).